

Gold Nanoparticles Coated with SH-PEG-NH₂ and Loaded with Ziyuglycoside I for Promoting Autophagy in Hematopoietic Stem Cells

Yongai Xiong^{1,2}, Tingting Chen^{1,2}, Lei Chen^{1,2}, Rongshan Cai^{1,2}

¹Key Laboratory of Basic Pharmacology of Guizhou Province and School of Pharmacy, Zunyi Medical University, Zunyi, Guizhou, 563000, People's Republic of China; ²Key Laboratory of Basic Pharmacology of Ministry of Education and Joint International Research Laboratory of Ethnomedicine of Ministry of Education, Zunyi Medical University, Zunyi, Guizhou, 563000, People's Republic of China

Correspondence: Yongai Xiong, Email yaxiong@zmu.edu.cn

Introduction: Radiotherapy and chemotherapy are the fundamental causes of myelosuppression in cancer patients, which usually induce a serious hematopoietic system toxicity, causing the hemocytes and immunity decline of patients. Ziyuglycoside I (ZgI), an active ingredient isolated from traditional Chinese medicine *Sanguisorba officinalis* L, has been demonstrated to increase the leucocytes and protect hematopoietic stem cells, which is related to its promotion of autophagy in hematopoietic stem cells.

Methods: In the present study, we formulated the SH-PEG-NH₂-coated gold nanoparticles loading ZgI (ZgI-AuNPs) with a enhanced autophagy promotion in hematopoietic stem cells. ZgI-AuNPs were prepared by HAuCl₄-sodium citrate reduction method, and the synthesis of ZgI-AuNPs was validated by XRD, FT-IR, DSC, and TEM findings. Furthermore, the drug loading rate and the release of ZgI were evaluated, and the ZgI-AuNPs' effects on autophagy and immunofluorescence staining for LC3B were tested. Finally, the effect of ZgI-AuNPs on the autophagy and hematopoietic ability of HSCs in vivo was also carried out.

Results: The prepared ZgI-AuNPs have an irregular cubic crystal structure by TEM observation, and the average particle size was 340 ± 16.5 nm determined by DLS. The XRD, FT-IR and DSC detection showed that the ZgI had been well loaded in AuNPs, and the AuNPs can load the ZgI at a content of 160.63 ± 1.35 μg·mg⁻¹. Meanwhile, the AuNPs can reduce the drug release rate of ZgI. Importantly, the ZgI-AuNPs enhanced autophagy of HSCs both in vitro and in vivo. At the same time, the gold nanoparticles enhance the hematopoietic effect of ZgI on mice HSCs.

Conclusion: Our research suggests that SH-PEG-NH₂-coated gold nanoparticles loading ZgI has potential application in myelosuppression therapy.

Keywords: myelosuppression, HSCS, autophagy, gold nanoparticles, Ziyuglycoside I

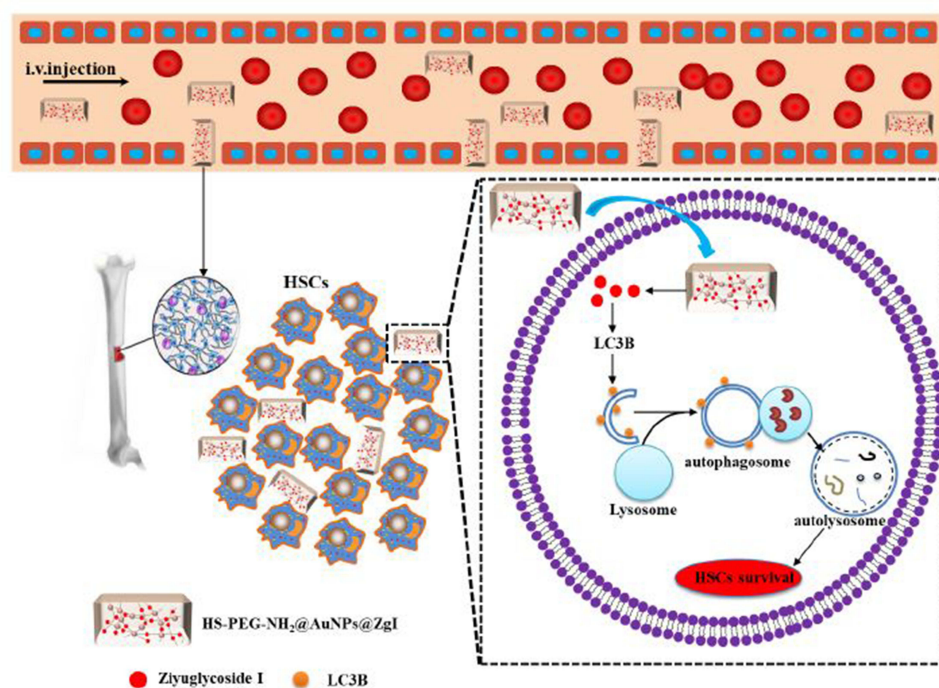
Introduction

Myelosuppression is a severe adverse reaction caused by chemotherapy and radiotherapy that might affect patients receiving treatment for malignancies. A decrease in peripheral blood hemocyte counts, including leucocyte, erythrocyte, platelet, and neutrophil counts, is the classic indicator of myelosuppression. This frequently causes infection, bleeding, or anemia in cancer patients. To end myelosuppression, effective therapeutic options are urgently needed.^{1,2}

In recent years, autophagy has been shown to play an important role in the life course of haematopoietic stem cells (HSCS), which is closely associated to the properties of HSCS (self-renewal,³ pluripotency,⁴ differentiation,⁵ and resting state).⁶ Both Jacquelin et al and Warr et al^{7,8} showed that autophagy is also an HSCS survival mechanism under radiotherapy and chemotherapy harm. Additionally, cytoprotective autophagy can increase HSCS's ionizing radiation tolerance. It is clear that autophagy is crucial for maintaining the HSCS's life processes and activities. In order to increase hematopoietic stem cells' resistance to chemoradiotherapy, it is crucial to increase autophagy in these cells.

Ziyuglycoside I (ZgI) is an active component extracted from the traditional Chinese medicinal *Sanguisorba officinalis* L, it increases leucocytes and protects hematopoietic stem cells.⁹ In a recent work, we found that ZgI can drastically

Graphical Abstract



downregulate the expression of mTOR protein in HSCs in myelosuppressed mice while significantly upregulating the expression of Atg5, Atg7, Beclin-1, LC3B, and other proteins in HSCs.¹⁰ What's more, we simulated the molecular docking of ZgI and mTOR by computer. It was found that ZgI and mTOR could bind well, and multiple hydroxyl groups in ZgI structure interacted with LYS105, GLY101, LYS89 and ASN39 in mTOR kinase to generate multiple hydrogen bonds, as shown in Figure 1. This interaction increased the binding force between ZgI and mTOR protein. It has been hypothesized that ZgI may be an autophagy activator, and that its ability to increase leukocytes and defend HSCs may be connected to encouraging HSC autophagy. However, previous studies have shown that ZgI has poor water solubility and low oral bioavailability, which may adversely affect its efficacy.¹¹ Therefore, modern preparation methods are needed to improve the above problems in order to improve its efficacy and activity.

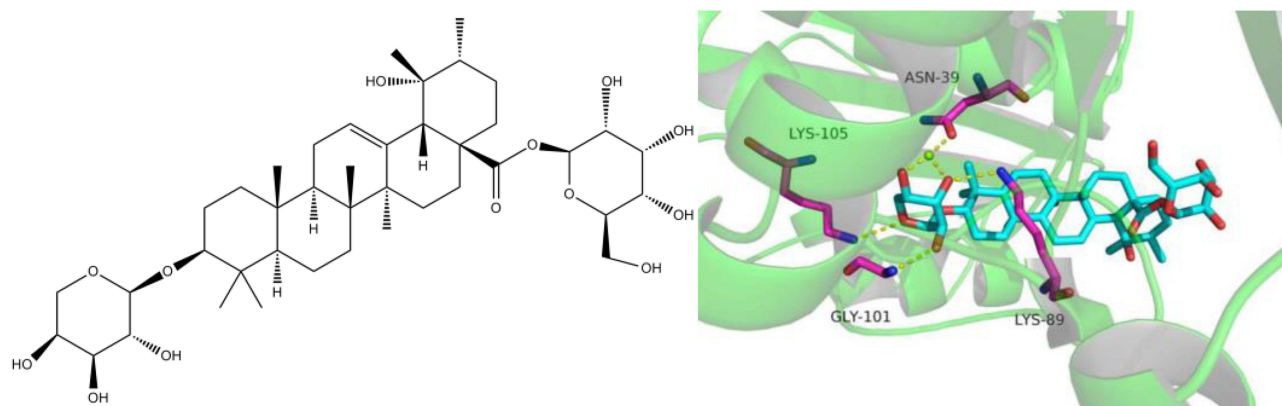


Figure 1 The chemical structure of Ziyuglycoside I its interaction with mTOR.

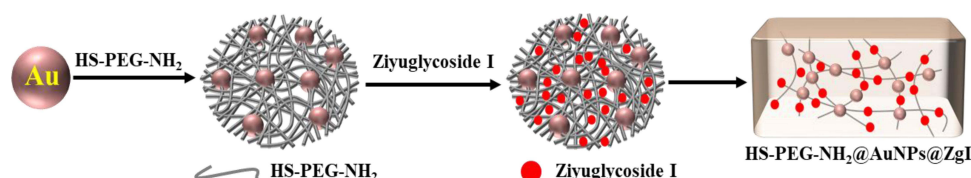


Figure 2 Preparation scheme of Zgl-AuNPs.

AuNPs (Gold nanoparticles, AuNPs), as a new type of drug delivery system, are widely used in the field of pharmacy due to their good biocompatibility, targeting, and easy surface modification.^{12,13} In addition, studies have confirmed that AuNPs is an autophagy regulator that can promote autophagy.^{14,15} Hence, it can be used as drug carriers to enhance autophagy. Therefore, we chose AuNPs as the carrier of Zgl in order to enhance the protective autophagy of HSCs.

This paper aims to covalently combine Zgl and gold nanoparticles to create Zgl-AuNPs, as is shown in Figure 2, and study its effect on autophagy in HSCs. This is based on the previous research that Zgl protects HSCs by regulating autophagy, combined with the excellent biological properties of AuNPs and the promotion of autophagy.

Materials and Cell Lines

Ziyuglycoside I was purchased from MUST Biotech Co, Ltd. (Chengdu, China). Sodium citrate Regent Chemicals Co., LTD (Tianjin, China). Tetrachloroauric acid (HAuCl_4) was purchased from Sigma company. The SH-PEG- NH_2 was purchased from Aladdin Chemical Reagents Co., LTD (Beijing, China). The FBS and DMEM high-sugar medium were purchased from Gibco (USA). The CCK-8 were purchased from Procell Life Science & Technology Co., Ltd (Wuhan, China). LC-3B and P62 antibody Kit was purchased from Abcam co.ltd (England). Cyclophosphamide (CTX) was kindly provided by Affiliated Hospital of Zunyi Medical University. Chloroquine (CLQ) was purchased from Sigma (USA).

Human hematopoietic stem cells (HSPC-1) cells were kindly provided by Procell Life Science & Technology Co., Ltd (Wuhan, China).

Preparation of Zgl-AuNPs

AuNPs were prepared by HAuCl_4 -sodium citrate reduction method.¹⁶ The optimized Zgl-AuNPs formula, (HAuCl_4 (1% w/w), sodium citrate (38.8mM), SH-PEG- NH_2 (0.25 mM), Zgl amount ($100\mu\text{g}\cdot\text{mL}^{-1}$), was the most convenient one with drug content of $15.63\mu\text{g}/\text{mg}$. Briefly, 38.8mM sodium citrate was added into 1% aqueous solution of HAuCl_4 , and the mixed solution was stirred on a magnetic stirrer for 6 hours to obtain gold nanoparticles (AuNPs), which was red colloid solution. Then 2.4 mL of 0.25 mM aqueous solution of SH-PEG- NH_2 was mixed with 6 mL of AuNPs colloid solution, and the mixed solution was supplemented with deionized water to 12 mL, stirring at room temperature for 30 min and putting it in a refrigerator at 4°C overnight. Then the Zgl of $100\mu\text{g}\cdot\text{mL}^{-1}$ was added and incubated in a constant temperature water bath at 37°C for 12 hours. The mixed solution was centrifuged for 30 minutes at a speed of 10,000 rpm to collect precipitates and remove the unreacted free Zgl after incubation.

Characterization of Zgl-AuNPs

At room temperature (25°C), a laser particle analyzer (90Plus PALS, Brookhaven, USA) was used to assess the zeta potential and particle size of Zgl-AuNPs. Prior to the assays, samples were ten times diluted in phosphate buffer solution ($\text{pH}=7.4$). Transmission electron microscopy (TEM, JEM-2100Plus; JEOL, Japan) and scanning electron microscopy (SEM, S4800; HITACHI, Japan) were used to detect the morphology of Zgl-AuNPs.

Thermo Fisher Scientific, USA) used ultraviolet spectrometry to measure the drug loading (DL) and encapsulation efficiency (EE) of Zgl-AuNPs.¹⁷ In a nutshell, PBS was used to dissolve the Zgl-AuNPs powder, and the absorbance of Zgl was measured at 204 nm. The Thermo Fisher, USA's Nicolet 6700 Fourier transform infrared spectroscopy was employed to ascertain Zgl's physical condition inside the AuNPs. The pristine Zgl, physical mixture of Zgl and AuNPs and Zgl-AuNPs were detected and compared.

Radiation Diffraction (XRD). The structural features of the materials were determined using a D8 Focus X-ray diffractometer from Bruker in Germany that was equipped with Cu-K radiation. The voltage and current used for the experiments were 35 kV and 40 mA. From 5° to 90°, samples were scanned at a rate of 6°/min.

Analysis using a differential scanning calorimeter (DSC). A DSC 250 differential scanning calorimeter (TA Instruments, USA) was used for DSC. Before testing, samples were placed in an aluminum sample pan and dried at 60 °C for 1 hour. The analysis was conducted with a flow rate of 20 mL/min and a heating rate of 10 °C/min in a nitrogen environment. In the temperature range of −40 °C to 400 °C, the thermogram was recorded.

Cell Culture and Cell Viability Assay

In order to support the development of CD34⁺ hematopoietic stem cells, HSPC-1 cells were cultivated in RPMI-1640 with 10% fetal bovine serum along with 100 U/mL of penicillin and 100 g/mL of streptomycin. By using the CCK-8 assay, the cytotoxicity of ZgI-AuNPs was evaluated. By measuring absorbance at 450 nm in a microplate reader, the OD values were determined (MK3, Thermo, USA).

In vitro Release

The in vitro release of ZgI and ZgI-AuNPs was carried out on a thermostatic oscillator (Changzhou Enpei Instrument Manufacturing Co., LTD, China). The ZgI and ZgI-AuNPs were dispersed in water, shaking at a speed of 100 r·min^{−1} and at a temperature of (37±0.5) °C. 1 mL release medium was taken out at 0.5, 2, 4, 6, 8, 10, 12, 24, 36 and 48 h. Then the release medium was centrifuged at 10,000 r·min^{−1} for 15 min and the absorbance of supernate was measured at 254 nm. At the same time, equal volume of isothermal release medium was replenished. The cumulative drug release rate (Q) at different time points was calculated according to following formula, and the cumulative release curve was drawn.

$$Q = \frac{c_n V_0 + \sum_{i=1}^{n-1} c_i V_i}{m} \times 100\%$$

Where V_0 is the total volume of the release medium (mL), C_i and C_n are the drug concentration (mg·mL^{−1}) measured at the i-hr and n-hr time points, V_i is the sampling volume (mL), and m is the total mass of ZgI in the samples.

Effect of ZgI-AuNPs on the Autophagy of HSPS in vitro

Hematopoietic stem cells were injured in vitro using the chemotherapy drug cyclophosphamide (CTX). A 96-well plate containing HSPC-1 cells was seeded with 1×10^5 cells per well. The settings for the experimental groups were the normal control group (NC, saline + RPMI 1640), CTX (CTX + RPMI 1640), ZgI and ZgI-AuNPs treatment group (CTX + RPMI 1640 supplemented with ZgI and ZgI-AuNPs of 5 µg·mL^{−1} concentration, respectively). CTX was applied to cells in all other groups excluding the NC group at a concentration of 1 M. After 36 hours of incubation, the supernatant from each group was collected, and the appropriate drugs were then added. Cell viability was assessed after a 24-hour treatment using the CCK-8 test.

TEM was used to study the autophagy condition of HSPC-1 cells. The HSPC-1 cells were rinsed with PBS, fixed for 4 hours in 2.5% glutaraldehyde in PBS, and then post-fixed for another 2 hours in 1% OsO₄ in PBS. The samples were dried using ethanol gradients before being transferred to absolute acetone for 20 minutes. The samples were placed in a 1:1 mixture of absolute acetone and the final Spurr resin (SPI-CHEM, 02690-AB) mixture for one hour at room temperature, then moved to a 1:3 mixture of absolute acetone and the final resin mixture for three hours, and finally to the final Spurr resin mixture for an overnight period. Under transmission electron microscopy, the ultrastructures of the cells were studied.

By using immunofluorescence analysis, the protein LC3B that is connected to autophagy was detected. In a nutshell, HSPC-1 cells were washed in PBS, fixed for 20 min at room temperature with 4% paraformaldehyde, and then permeabilized for 10 min with Triton X-100 (Solarbio, T8200). Cells were first blocked for 1 hour with the immunostaining blocking buffer (Beyotime Biotechnology, P0252), and then treated with primary Anti-LC3B (Abcam, ab192890, 1:1000) antibodies overnight at 4°C. The secondary goat anti-rabbit antibodies (Solarbio, SE134; 1:1000) were incubated for 1 hour at room temperature. DAPI (Solarbio, C0065) was used to stain the nuclei for five minutes at room

temperature. Finally, cells from each group were examined using a fluorescent microscope (CKX53IPC; Olympus, Japan), and the accompanying cellsens standard software was used to calculate the relative fluorescence intensity.

Effect of Zgl-AuNPs on the Autophagy of HSPs in vivo

SPF grade male and female KM mice (aged 5 weeks, weighing 20 ± 2 g) were purchased from Tianqing Biotechnology Co., Ltd of Changsha (Changsha, China). Animals were individually housed in SPF facilities during the experiment. All of the animal experimental protocols were approved by the Ethics Committee of Zunyi Medical University. All animal care and experimental procedures were performed in accordance with the Laboratory Animal Welfare and Ethics Committee of China.

Autophagy suppression model: Mice were injected with CTX (120 mg/kg) or Chloroquine (CLQ, 60 mg/kg) normal saline solution intraperitoneally to make autophagy suppression model. Mice were randomized into six groups with 10 mice in each group, including Normal control group (NC group), CTX group, CLQ group, CTX+CLQ group, Zgl (20mg/kg) + CTX+CLQ group and Zgl-AuNPs (20mg/kg, containing Zgl 64.25 μ g) +CTX+CLQ group. Except the mice of NC group, mice in the other groups were injected with CTX or CLQ intraperitoneally. Mice in Zgl group and Zgl-AuNPs group were injected with 0.2mL Zgl and Zgl-AuNPs PBS solution via tail vein, respectively.

The CTX was injected one time at the first day of experiment. The CLQ was injected at the first, third and fifth day, respectively. The body weights and survival rate in each group were monitored daily for 6 days. At day 6 p.i., blood samples of each group were collected by retro-orbital puncture into heparinized tubes, the leucocyte and neutrophils were assayed by automatic blood cell counting instrument (URIT-3000, Shanghai, China). The bone marrow cell suspension was obtained by crushing mice bones (femurs and tibias) in PBS containing 2% FBS and filtering it through a 70mm cell strainer. Red blood cells were lysed by ammonium chloride solution to get the bone marrow cell suspension. As described earlier,¹⁸ Ckit⁺ cells were enriched for Ckit by MACS (MiltenyiBiotec) using anti-Ckit magnetic beads, and HSCs were sorted using a BD FACS Aria Fusion (BD Biosciences). The autophagy state of Ckit⁺ cells was observed by TEM.

Immunohistochemical Analysis

Mice HSCs were paraffin-embedded and sectioned, endogenous enzymes were inactivated, antigens were thermally repaired and the anti-P62 antibody was added (1:100 dilution) for 1 h at 37 °C. Then the anti-rabbit IgG (1:50 dilution) was added and incubated at 37 °C for 1 h. After that, the DAB was used for colour development, and the hematoxylin was used for restaining. Finally, the Image Pro Plus 6.0 image analysis software for semi-quantitative analysis of P62 expression in mice HSCs.

Statistical Analysis

All the data in this study were analyzed by SPSS 19.0. Data are expressed as mean \pm SD. For values that were normally distributed, direct comparison between two groups was conducted by Independent Sample's *t*-test. *P* value of < 0.05 was considered statistically significant.

Results

Characterization of Zgl-AuNPs

The preparation process of Zgl-AuNPs was briefly shown in Figure 3A, and the samples were characterized by particle size distribution, SEM, TEM, FTIR, DSC and XRD. From the Figure 3B we can see that the average particle size of Zgl-AuNPs is (340 ± 16.5) nm, and the zeta-potential measurements showed that the produced Zgl-AuNPs had a charge of -35.49 ± 1.59 mV. In the water solution, the AuNPs had λ_{\max} of absorption at 525 nm, while the Zgl-AuNPs had λ_{\max} of absorption at 254 nm and 525 nm, respectively, preliminarily confirming the formation of Zgl-AuNPs (Figure 3C). In addition, the Zgl-AuNPs have an irregular cubic crystal structure (Figure 3D and E).

The FTIR analysis (Figure 4) showed that the characteristic peaks of Zgl are mainly at 3430, 2927, 1732, 1634, 1456, and 1073 cm^{-1} , corresponding to -OH stretching vibration, CH_2 antisymmetric stretching, C=O stretching vibration, C=C

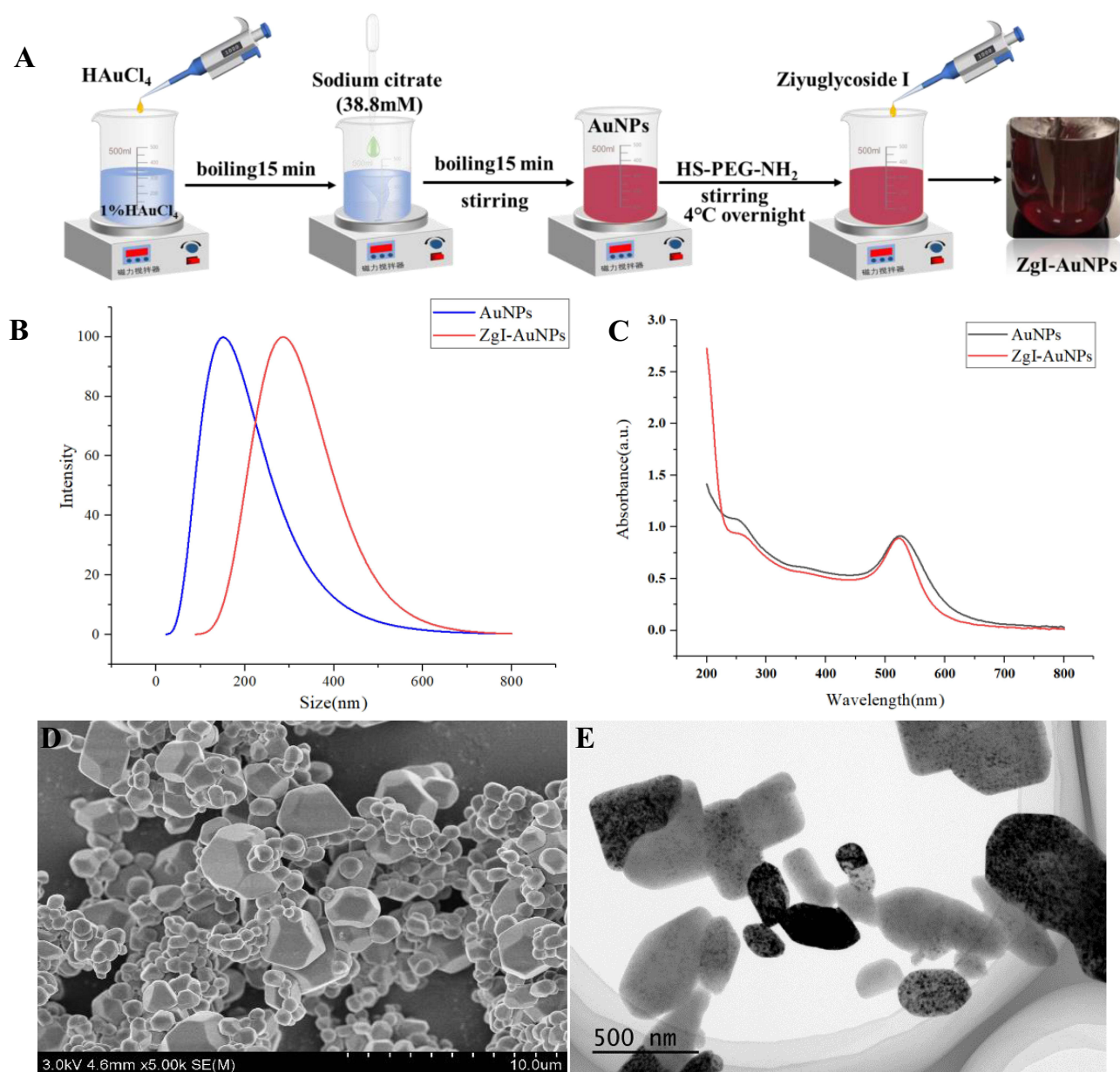


Figure 3 The preparation and characterization of ZgI-AuNPs. **(A)** The brief illustration of ZgI-AuNPs preparation. **(B)** Size distribution of AuNPs and ZgI-AuNPs. **(C)** Absorbance spectra of AuNPs and ZgI-AuNPs. **(D)** TEM image. **(E)** SEM image.

stretching vibration, CH₂ deformation vibration and the stretching vibration of C-O, respectively. Compared with the physical mixture, AuNPs and ZgI-AuNPs, there are two characteristic absorption peaks on the spectrum, which located at 1732 and 1456 cm⁻¹, respectively. The physical mixture mainly has absorption peaks at 3406, 2930, 1635, 1419, and 1052 cm⁻¹, corresponding to -OH stretching vibration, CH₂ antisymmetric stretching, C=C stretching vibration, CH₂ deformation vibration and C-O stretching vibration, respectively. Compared with the spectrum of ZgI, the physical mixture also has the characteristic absorption peak of ZgI around 1456 cm⁻¹, but the characteristic absorption peak at 1732 cm⁻¹ disappears. ZgI-AuNPs mainly have absorption peaks at 3443, 2921, 1634, and 1070 cm⁻¹. Compared with the spectra of ZgI and physical mixtures, the characteristic absorption peaks of ZgI-AuNPs at 1732 and 1456 cm⁻¹ disappear. The FTIR detection indicated that the ZgI had been loaded in AuNPs.

Figure 5 illustrates the DSC thermogram of ZgI-AuNPs in comparison with the thermograms of ZgI alone and AuNPs alone. The thermogram of ZgI alone has two distinct characteristic peaks at 140.41 and 187.10°C, respectively. The

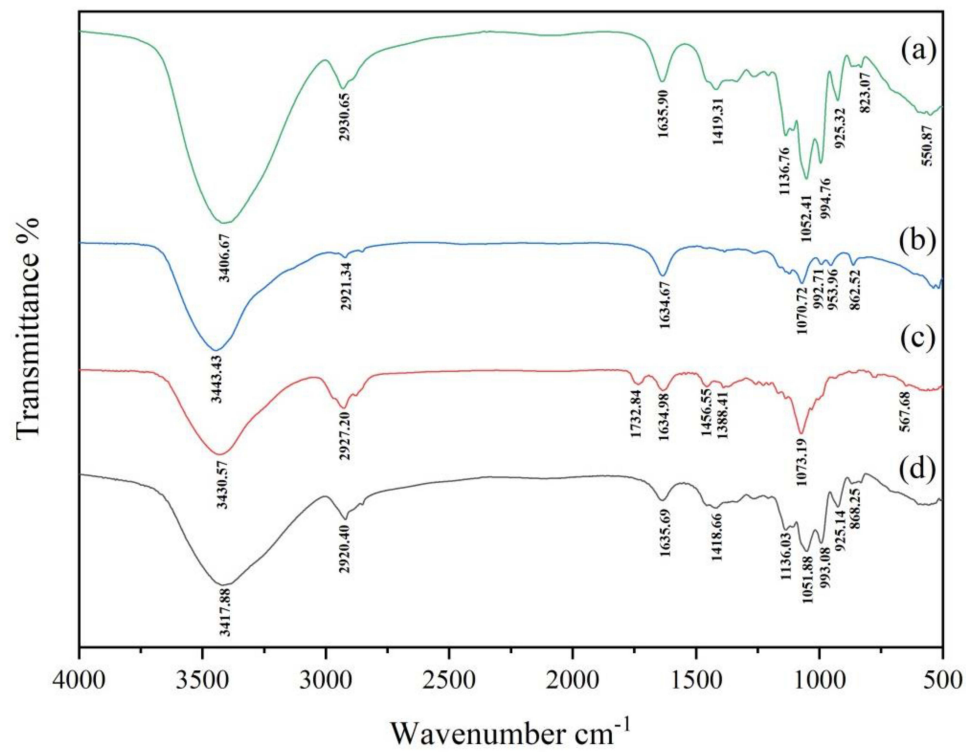


Figure 4 The FTIR spectrum. (a) Physical mixture. (b) Zgl-AuNPs. (c) Zgl. (d) AuNPs.

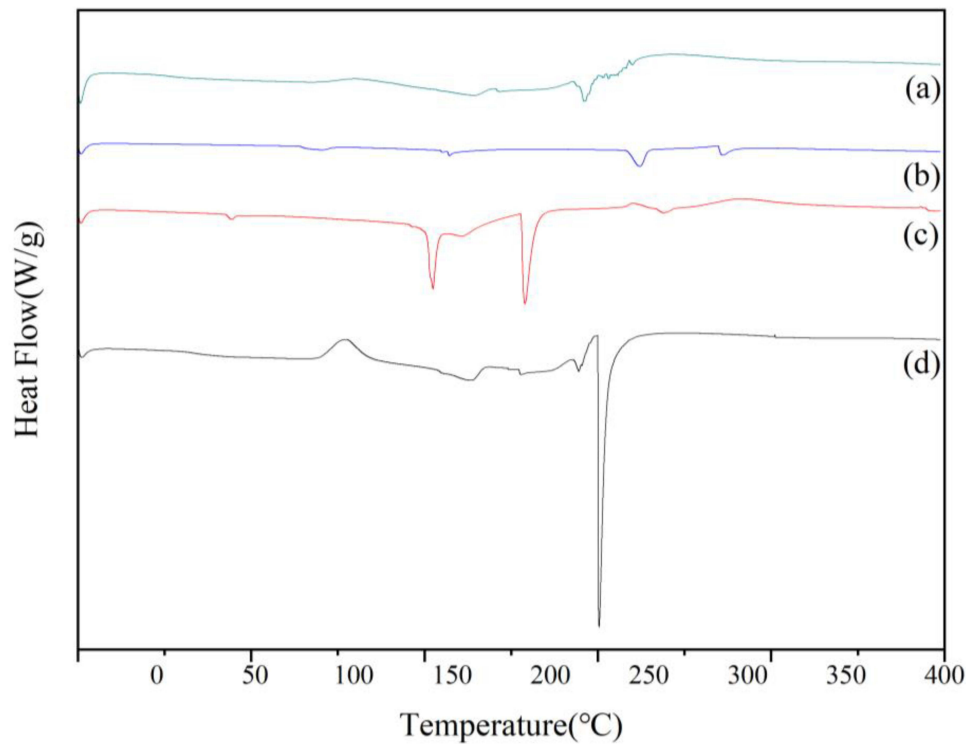


Figure 5 The DSC thermogram. (a) Physical mixture. (b) Zgl-AuNPs. (c) Zgl. (d) AuNPs.

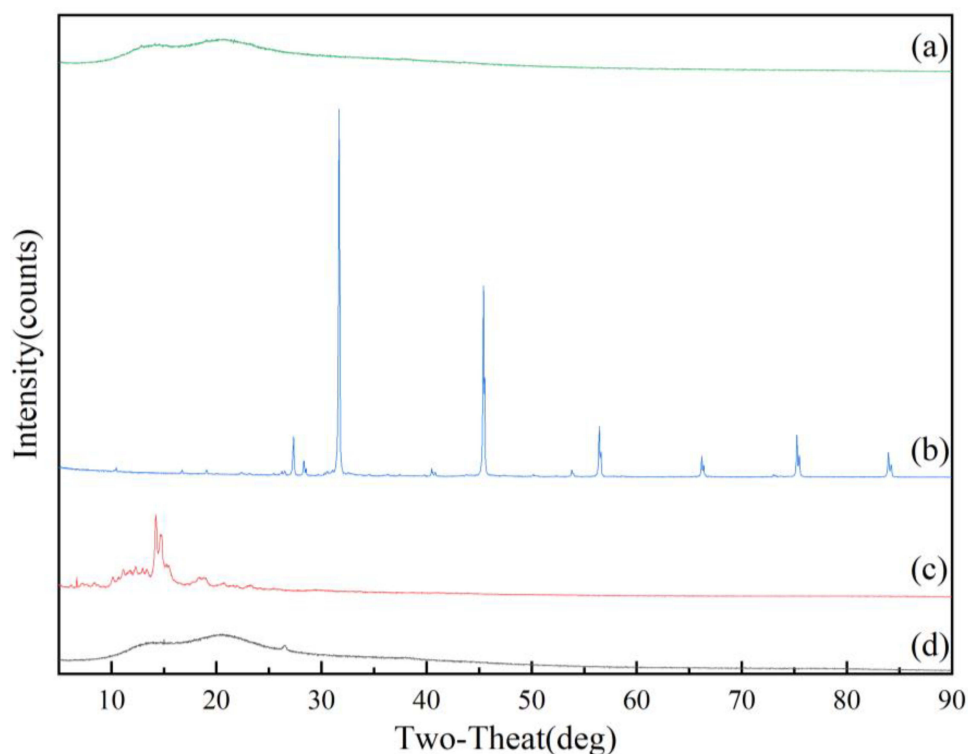


Figure 6 The XRD spectrum. (a) Physical mixture. (b) Zgl-AuNPs. (c) Zgl. (d) AuNPs.

thermogram of AuNPs alone has one distinct characteristic peak at 224.72°C. The thermogram of physical mixture has two characteristic peaks at 159.34 and 217.99°C, respectively. The thermogram of Zgl-AuNPs has four characteristic peaks at 82.92, 148.65, 245.49 and 287.46 °C, respectively. The two characteristic peaks of the physical mixture are close to the characteristic peaks of Zgl and AuNPs alone, respectively, indicating that there are pure Zgl and AuNPs in the physical mixture. It is speculated that simple physical mixing cannot change the state of Zgl and AuNPs. In the spectrum of Zgl-AuNPs, it can be seen that its characteristic peaks not only appear near the characteristic peaks of Zgl and AuNPs, but also other peaks appear in the spectrum. It is speculated that the combination of Zgl and PEG-modified AuNPs caused the change of the peaks.

The XRD patterns of AuNPs and Zgl-AuNPs are shown in Figure 6. The diffraction pattern of Zgl showed a significant number of peaks between 10 ° and 20 °, indicating that Zgl is crystalline. In conformity with the pure crystalline gold standard PDF card (PDF#99-0056), the pure AuNPs exhibit five distinctive peaks at 38.18°, 44.38°, 64.57°, 77.56°, and 81.72°, respectively. No other noticeable impurity peaks also emerged. The diffraction peaks of Zgl vanish from the spectrum, and the distinctive peaks of Zgl-AuNPs appear at 31.72°, 45.43°, 66.14°, 76.56°, and 84.11°, respectively, which correspond to the gold standard PDF card. It is assumed that Zgl-AuNPs were prepared successfully.

Drug Loading Capacity

The drug loading capacity of Zgl loaded in the AuNPs were $160.63 \pm 1.35 \mu\text{g} \cdot \text{mg}^{-1}$ and the encapsulation efficiency of Zgl reached to $(91.29 \pm 3.48)\%$. As shown in Table 1.

Table 1 The DL and EE of Zgl-AuNPss
(n=3, mean±SD)

Samples	DL/ $\mu\text{g} \cdot \text{mg}^{-1}$	EE/%
Zgl-AuNPs	160.63 ± 1.35	91.29 ± 3.48

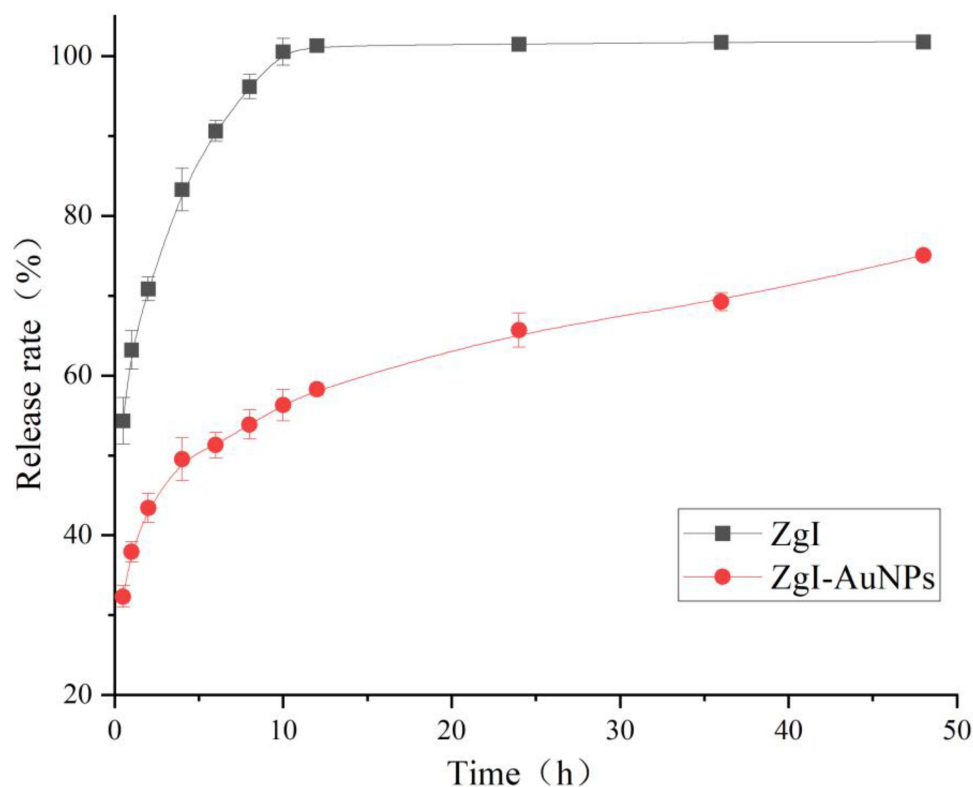


Figure 7 The test result of cumulative ZgI release. Data are presented as mean \pm SD from three independent experiments.

In vitro ZgI Release Test

Figure 7 showed the cumulative release rate of pristine ZgI and ZgI-AuNPs in water. Compared with the pristine ZgI, drug in AuNPs exhibited more slowly release rate, showing a sustained release. In the presented result we can see that approximate 100% of pristine ZgI was released at 10h, while the ZgI release in ZgI-AuNPs is only (56.30 \pm 1.97) % at the same point. At 48 h, the cumulative release of ZgI was (75.07 \pm 0.23) % for ZgI-AuNPs. The result suggested that ZgI-AuNPs exhibited a slower drug release rate than that of ZgI.

Cytotoxicity in vitro

Cytotoxicity of CTX and ZgI-AuNPs were evaluated by the CCK-8 assay in vitro. The result showed that the effect of different concentrations of CTX on the survival rate of HSCS varies greatly. The survival rate of HSCS steadily declines as CTX concentration rises. According to Figure 8A, the survival rate of HSCS is near to 50% when CTX concentration is 0.125 μ M. The best concentration to cause HSCS damage was therefore CTX at a concentration of 0.125 M. As demonstrated in Figure 8B, ZgI-AuNPs had no impact on the activity of HSCS in the concentration range of 5–160 μ g \cdot mL⁻¹, and all six experimental groups exhibited HSCS cell viability levels above 90%. The ZgI-AuNPs with a concentration of 5 μ g \cdot mL⁻¹ was finally selected as the optimal administration concentration.

Effects on the Autophagy in HSCs in vitro

As shown in Figure 9A, TEM showed many autophagosomes, as shown by the yellow arrow, with a distinct double membrane structure in the normal group cells, but this structure was either absent in the cells of model group (Figure 9B), suggesting that the CTX weakened the autophagy in HSCs. A small number of autophagosomes can be observed in the AuNPs group cells (Figure 9C), and autophagosomes can also be observed in the cells of ZgI group (Figure 9D). However, there were significantly more autophagosomes in the cells of ZgI-AuNPs group compared with

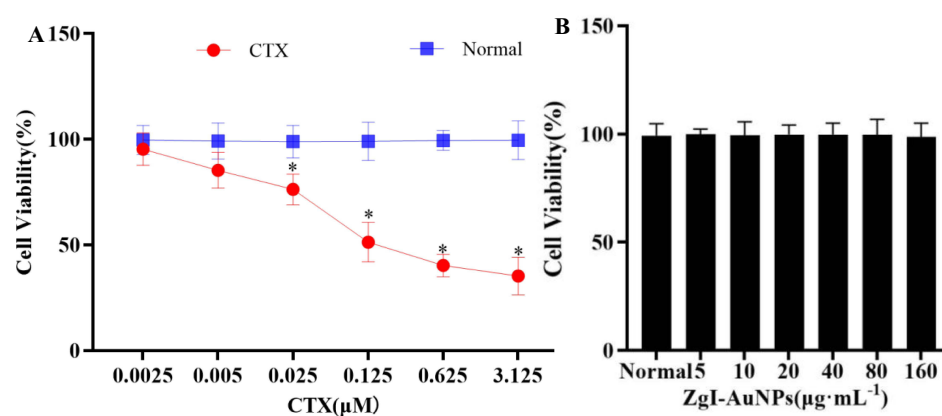


Figure 8 The effect of Zgl-AuNPs on survival rate of HSCs. (A). The cytotoxicity of CTX in normal HSPC-I cells (n = 3, Mean ± SD). (vs Normal, * $P < 0.05$, ** $P < 0.05$). (B). The viability of HSPC-I cells.

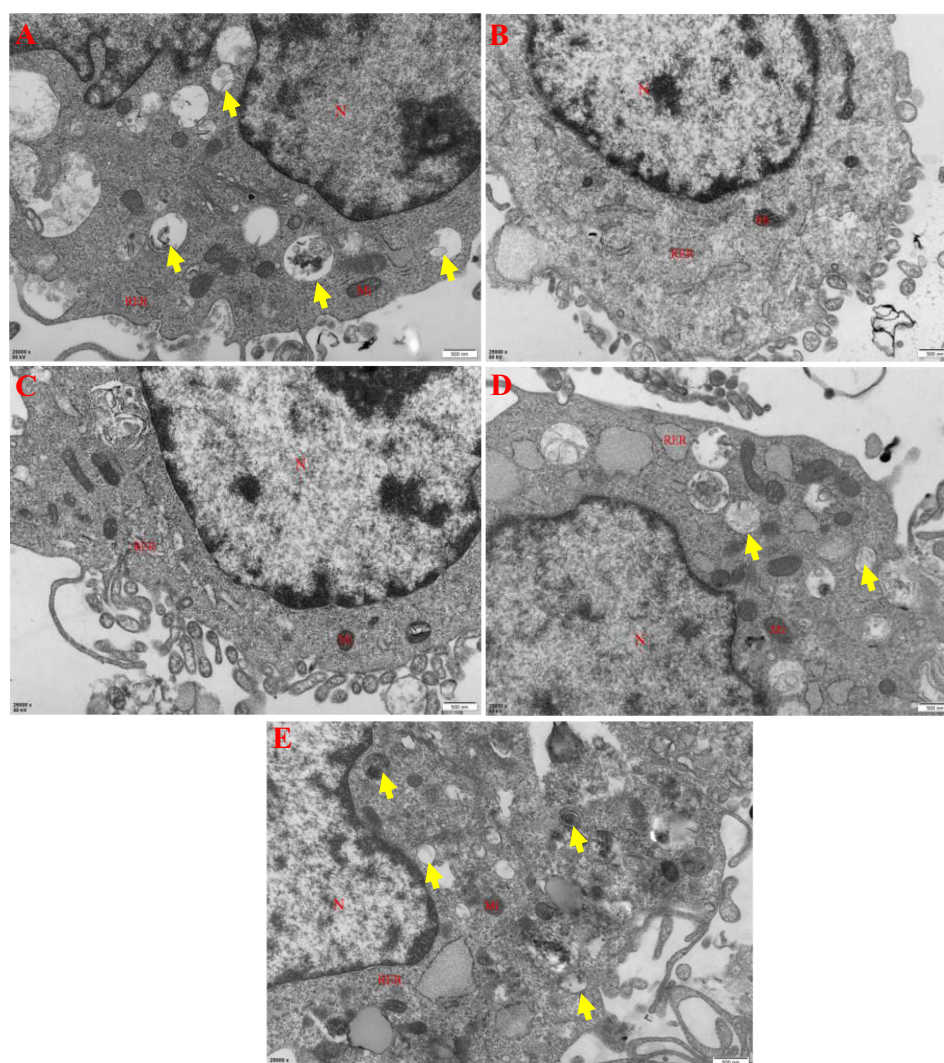


Figure 9 The effect of Zgl-AuNPs on the autophagy of HSCs cells. The red labeling of "N" represents the cell nuclear, the "Mi" represents the mitochondria and the "RER" represents the rough endoplasmic reticulum. The yellow arrows represents the autophagosomes. (A). Normal group: saline + RPMI 1640. (B). Model group: CTX + RPMI 1640. (C). AuNPs group: CTX + AuNPs. (D). Zgl group: CTX + Zgl. (E). Zgl-AuNPs group: CTX + Zgl + AuNPs.

the cells of model, AuNPs and Zgl group (Figure 9E), indicating that the activity of Zgl promoting autophagy of HSCs was enhanced by gold nanoparticles.

To further confirm the effect of gold nanoparticles on the Zgl, the LC3B, an important marker protein of autophagy was detected in HSCs of each group. According to Figure 10A, the fluorescence intensity of LC3B in the HSCs of the model group and Zgl group was significantly lower than that of the normal group ($P < 0.01$), indicating that the degree of autophagy in HSCs was greatly reduced following CTX injury. The fluorescence intensity of LC3B in the HSCs of the

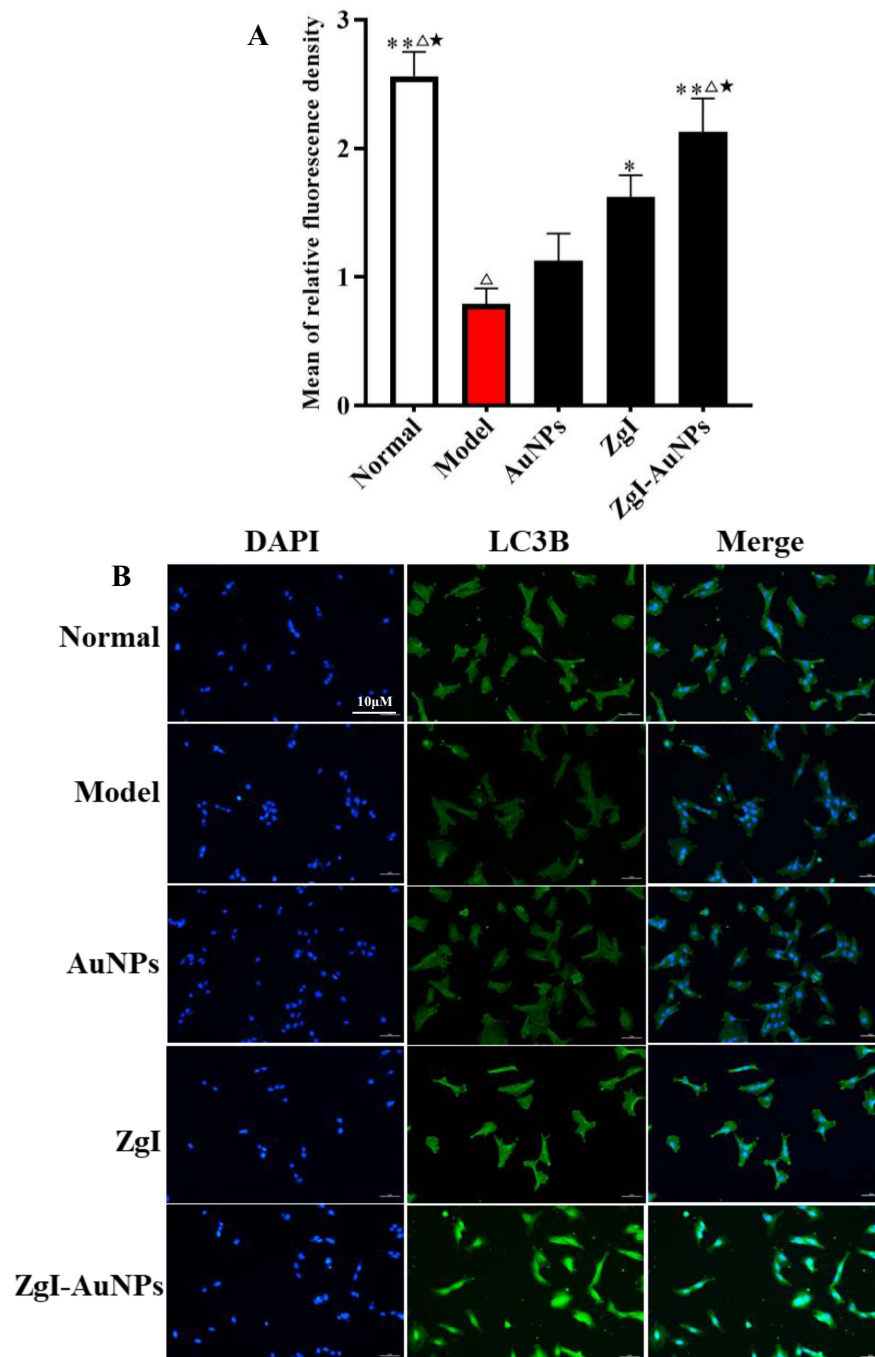


Figure 10 The effect of Zgl-AuNPs on the expression of LC3B in HSC cells. **(A)** The mean of relative fluorescence density. **(B)** The green fluorescence of LC3B photographed by fluorescence microscope. Normal group: saline + RPMI 1640. Model group: CTX + RPMI 1640. AuNPs group: CTX + AuNPs. Zgl group: CTX + Zgl. Zgl-AuNPs group: CTX + Zgl- AuNPs. Data are presented as mean \pm SD from six independent experiments (vs model group, * $P < 0.05$, ** $P < 0.05$; vs AuNPs, $^{\Delta}P < 0.05$, $^{\Delta\Delta}P < 0.01$; vs Zgl, * $P < 0.05$, ** $P < 0.01$).

ZgI group was significantly increased ($P < 0.05$) when compared to the model group, and it was dramatically increased ($P < 0.01$) when ZgI-AuNPs administration was used. The fluorescence intensity of LC3B in the HSCs of the ZgI-AuNPs group was likewise considerably higher than that of the ZgI group at the same time ($P < 0.05$), demonstrating that AuNPs improved ZgI's inhibitory effect on the decline in autophagy in HSCs brought on by CTX. Figure 10B displays the immunofluorescence detection of LC3B in the HSCs of each experimental group.

Effects on the Autophagy and Hematopoietic Function of HSCs in vivo

In vivo experiments also confirmed that the ZgI-AuNPs significantly promoted autophagy in HSCs. From the Figure 11A we can see that a large number of autophagic lysosomes and autophagic vesicles are present in haematopoietic stem cells which maintain the normal haematopoietic function. Both the CTX and CLQ damaged autophagy in mice HSCs, inducing a significant decrease in autophagosomes and autophagic vesicles, as shown in Figure 11B and C. The autophagy of mice HSCs was more severely disturbed when CTX and CLQ were coupled, and autophagosomes and autophagic vesicles were hardly visible under transmission microscopy, as illustrated in Figure 11D. ZgI could partially protect mice HSCs from the autophagic degradation caused by CTX and CLQ, and few autophagosomes were seen in the ZgI group (Figure 11E). Numerous autophagosomes and autophagic vesicles were visible in mice HSCs treated with ZgI-AuNPs, which was in line with our anticipated outcome (Figure 11F). As a result, it was discovered that the gold nanoparticles enhanced ZgI's ability to promote autophagy in mouse HSCs.

Additionally, the immunohistochemical assay showed that P62 protein was significantly upregulated in mice hematopoietic stem cells after CTX and CLQ injection when compared with the normal group (Figure 12a), particularly in mice treated with the combination of CTX and CLQ, as shown in Figure 12b–d, respectively, suggesting that CTX and CLQ caused inhibition of autophagy in mice hematopoietic stem cells. Following ZgI and ZgI-AuNPs treatment, the P62

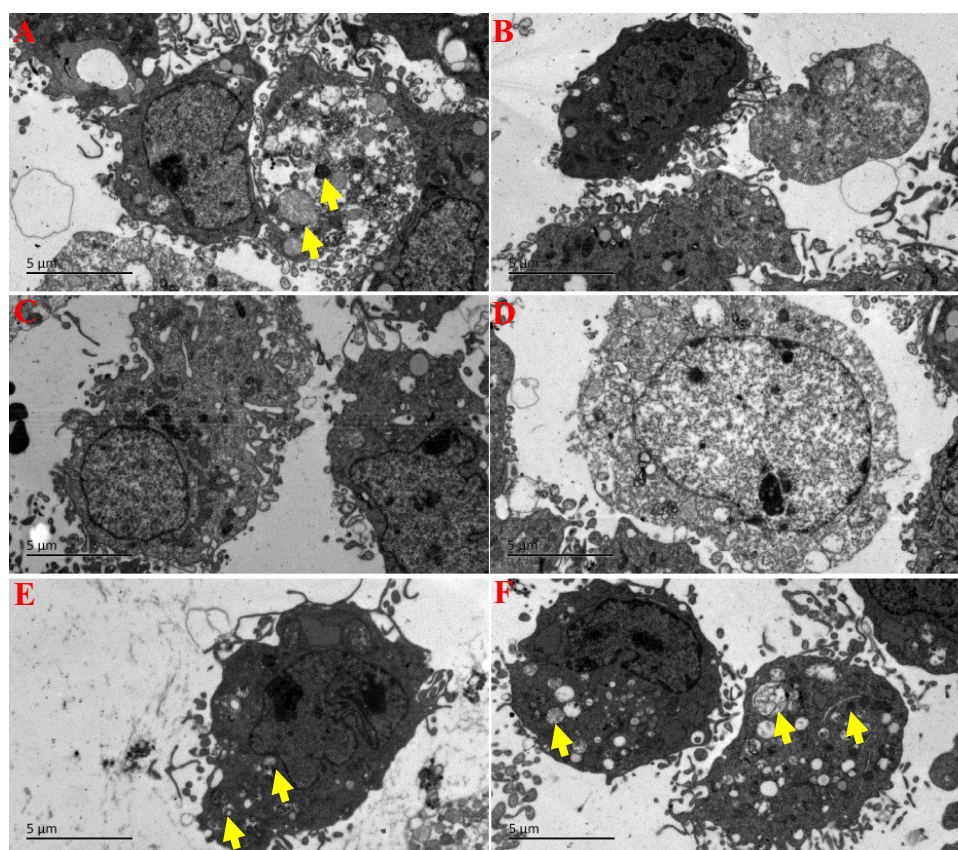


Figure 11 The effect of ZgI-AuNPs on the autophagy of mice HSCs cells. (A).NC group: saline. (B). CTX group:CTX + saline. (C). CLQ group: CLQ + saline. (D). CTX +CLQ group: CTX + CLQ + saline. (E). ZgI group: ZgI + CTX + CLQ + saline. (F).ZgI-AuNPs group: ZgI-AuNPs + CTX + CLQ + saline. The yellow arrows represents the autophagosomes.

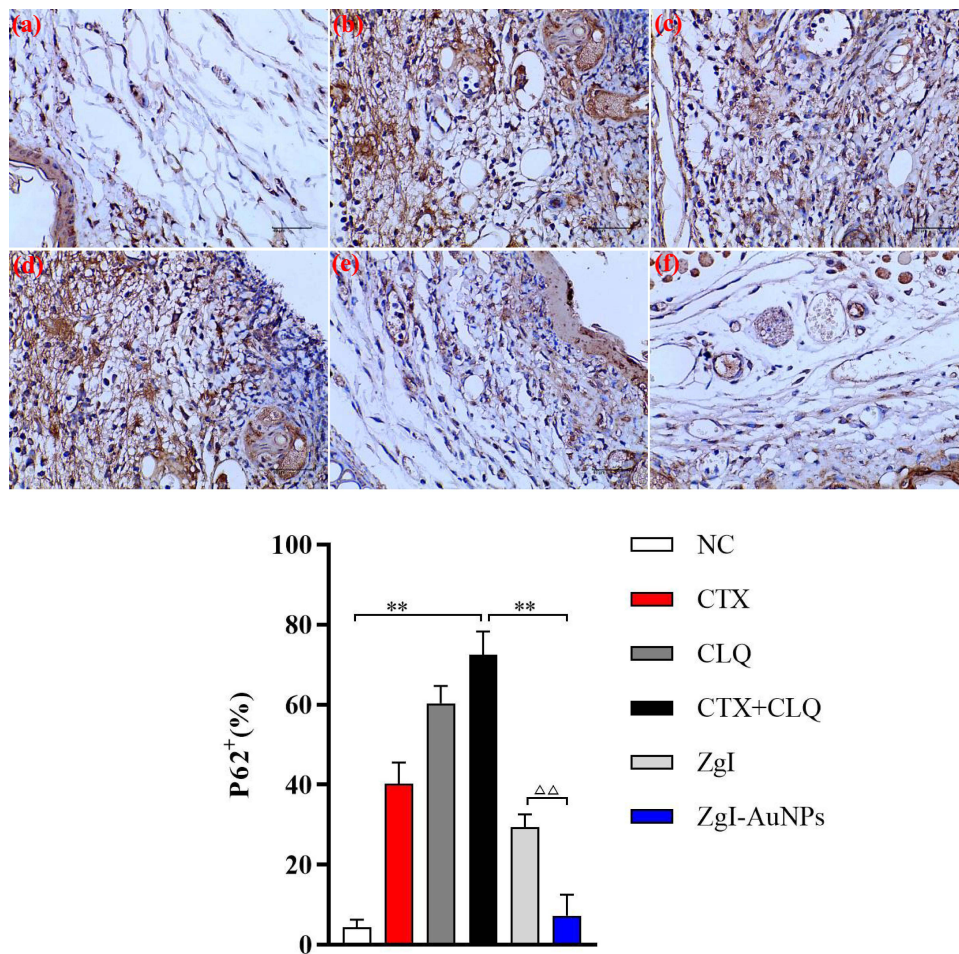


Figure 12 The immunohistochemical detection of P62 protein in hematopoietic stem cells. (A) The immunohistochemical images of P62 protein. (B) The statistical chart of P62 protein-positive cells. (a).NC group: saline. (b). CTX group:CTX + saline. (c). CLQ group: CLQ + saline. (d). CTX+CLQ group: CTX + CLQ + saline. (e). ZgI group: ZgI + CTX + CLQ + saline. (f).ZgI-AuNPs group: ZgI-AuNPs + CTX + CLQ + saline. Data are presented as mean \pm SD from six independent experiments (vs CTX+CLQ group group, * P <0.05, ** P <0.05; vs ZgI, $\Delta\Delta P$ < 0.01).

protein expression was considerably reduced in hematopoietic stem cells from mice, and ZgI-AuNPs-treated mice displayed a higher reduction in P62 protein expression than ZgI-treated mice, as shown in Figure 12e and f. It is suggested that ZgI can restore the autophagic destruction of hematopoietic stem cells induced by CTX and CLQ, and the gold nanoparticles can further enhance the autophagy-promoting effect of ZgI on hematopoietic stem cells.

Finally, we assessed the survival rate, body weight, and quantity of leukocytes and neutrophils in the peripheral blood of each experimental group to further support the beneficial effect of autophagy on the hematopoietic capacity of mice HSCs. Figure 13A and B show that mice injected with both CTX and CLQ experienced rapid weight loss starting on day three (P <0.05), and that the mortality rate significantly increased starting on day two, showing that mice are vulnerable to passing away when autophagy of HSCs is seriously disrupted. Leukocyte and neutrophil counts in the peripheral blood of mice given injections of CTX and CLQ were similarly dramatically decreased (P <0.01), as demonstrated in Figures 13C and D.

It suggests that mice HSCs' capacity to create leukocytes will be significantly reduced if their autophagy is eliminated. When mice were treated with ZgI-AuNPs, their body weight was well maintained (P <0.05), mortality was significantly reduced, and the number of leukocytes (P <0.01) and neutrophils (P <0.01) in peripheral blood was also significantly increased, and the above treatment effects were significantly better than those of ZgI treatment (P <0.05). It suggests that ZgI-AuNPs can effectively counteract the decline in HSCs' hematopoietic potential brought on by CTX and CLQ. At the same time, ZgI's hematopoietic effect on mice HSCs is strengthened by the gold nanoparticles.

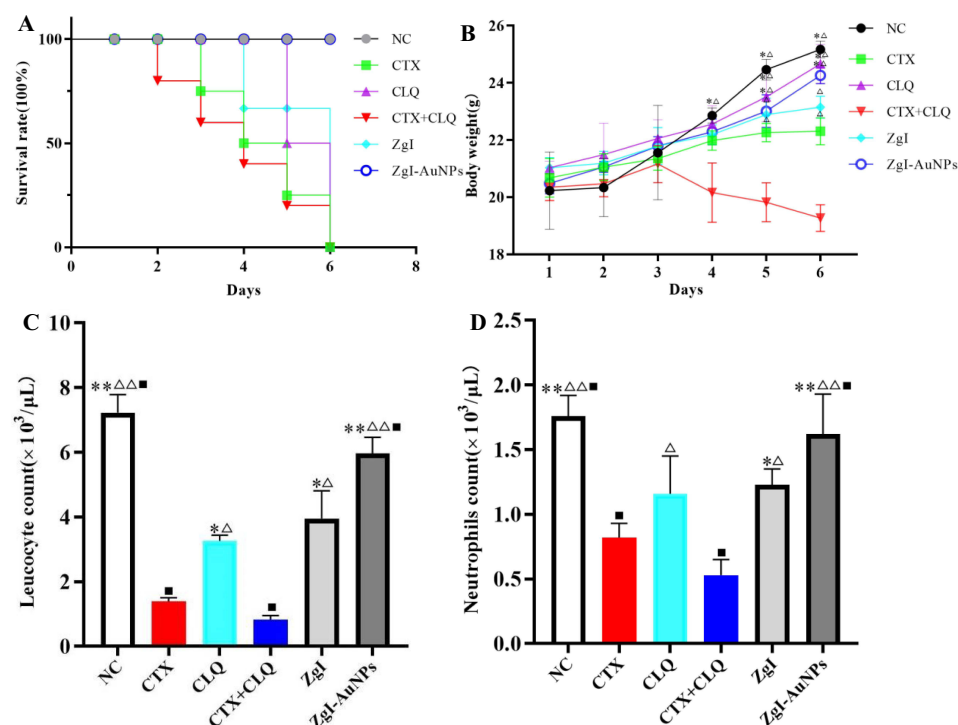


Figure 13 The effect of Zgl-AuNPs on the blood cell production capacity of mice HSCs. **(A)** The survival rate of each group. **(B)** The body weight change of each group ($n = 6$, Means \pm SD), (vs CTX group, $*P < 0.05$, $**P < 0.05$; vs CTX+CLQ group, $\Delta P < 0.05$, $\Delta\Delta P < 0.01$). **(C)** The leukocytes count of each group ($n = 6$, Means \pm SD), (vs CTX group, $*P < 0.05$, $**P < 0.05$; vs CTX+CLQ group, $\Delta P < 0.05$, $\Delta\Delta P < 0.01$; vs Zgl group, $^{\#}P < 0.05$). **(D)** The neutrophils count of each group ($n = 6$, Means \pm SD), (vs CTX group, $*P < 0.05$, $**P < 0.05$; vs CTX+CLQ group, $\Delta P < 0.05$, $\Delta\Delta P < 0.01$; vs Zgl group, $^{\#}P < 0.05$). NC group: saline. CTX group: CTX + saline. CLQ group: CLQ + saline. CTX+CLQ group: CTX + CLQ + saline. Zgl group: Zgl + CTX + CLQ + saline. Zgl-AuNPs group: Zgl-AuNPs + CTX + CLQ + saline.

Discussion

CTX is the most widely used alkylating agent antitumor drug in clinic, and it is also an immunosuppressant, which is often used in the treatment of various malignant tumors such as leukemia, lymphoma and breast cancer.¹⁹ In mice, CTX drastically decreased the number of blood cells, and it was initially verified that this was due to the damage CTX caused to the HSCs. This experimental investigation discovered that one key mechanism of CTX's harm to the body's hematopoietic system may be the loss of autophagy in HSCs produced by CTX. After excessive DNA damage from CTX's alkylation of cellular DNA or RNA, which impairs the ability of cells to repair themselves, autophagy is lost, which reduces the capacity of HSCs to self-renew and differentiate, which results in the development of hematological diseases. Further research is still needed to determine how exactly CTX suppresses autophagy in HSCs.

HSCs are the adult stem cells of the blood system that have the capacity for long-term self-renewal and the potential to differentiate into various types of mature blood cells.²⁰ Approximately one third of adult HSCs have a strong long-term regenerative potential similar to that of healthy young HSCs, exhibiting high levels of autophagy and a low metabolic state.²¹ Autophagy inhibits HSCs metabolism by removing active, healthy mitochondria, maintaining homeostasis and stemness, and maintaining the regenerative capacity of older HSCs becomes increasingly important as we age.²² Therefore, when the normal autophagy of HSCs is disrupted, the hematopoietic function of HSCs will be weakened and even cause the death of HSCs. In our study, we cannot observe autophagy in CTX and CLQ treated mice HSCs. The loss of autophagy in HSCs depletes leukocytes in the peripheral blood of mice and is also lethal to mice. The Zgl-AuNPs has a very significant protective and promotive effect on autophagy in mice HSCs, protecting them from destruction by CTX and CLQ and thus restoring the hematopoietic function of HSCs.

In brief, we have successfully formulated SH-PEG-NH₂-coated gold nanoparticles loading Ziyuglycoside I with a sustained drug release and enhanced autophagy of HSCs. Therefore, AuNPs can serve as Zgl carriers for the promotion of Zgl transcellular uptake and enhancement of pro-autophagy activity.

Conclusion

In this paper, we successfully developed a SH-PEG-NH₂-coated gold nanoparticles loading Ziyuglycoside I, which aimed to enhance the activity of ZgI promoting the autophagy of HSCs. The prepared ZgI-AuNPs have an irregular cubic crystal structure with an average particle size of (340 ± 16.5) nm. And the AuNPs can load the ZgI at a content of $160.63 \pm 1.35 \mu\text{g} \cdot \text{mg}^{-1}$. Meanwhile, the AuNPs can reduce the drug release rate of ZgI. The current study also showed the ZgI-AuNPs roles in promoting the autophagy of HSCs both in vitro and in vivo and enhancing the hematopoietic effect of ZgI on mice HSCs.

Author Contributions

All authors made a significant contribution to the work reported, whether that is in the conception, study design, execution, acquisition of data, analysis and interpretation, or in all these areas; took part in drafting, revising or critically reviewing the article; gave final approval of the version to be published; have agreed on the journal to which the article has been submitted; and agree to be accountable for all aspects of the work.

Funding

This work was supported by the National Natural Science Foundation of China (NO. 82260723) and the Science and Technology Support Program of Guizhou province (NO.[2021]Genaral410).

Disclosure

The authors declare no conflict of interest.

References

- Schirmacher V. From chemotherapy to biological therapy: a review of novel concepts to reduce the side effects of systemic cancer treatment (Review). *Int J Oncol*. 2019;54:407–419. doi:10.3892/ijo.2018.4661
- Zhang QY, Wang FX, Jia KK, Kong LD. Natural product interventions for chemotherapy and radiotherapy-induced side effects. *Front Pharmacol*. 2018;9:1253. doi:10.3389/fphar.2018.01253
- Gomez-Puerto MC, Folkerts H, Wierenga AT, et al. Autophagy proteins ATG5 and ATG7 are essential for the maintenance of human CD34(+) hematopoietic stem-progenitor cells. *Stem Cells*. 2016;34:1651–1663. doi:10.1002/stem.2347
- Phadwal K, Watson AS, Simon AK. Tightrope act: autophagy in stem cell renewal, differentiation, proliferation, and aging. *Cell Mol Life Sci*. 2013;70:89–103. doi:10.1007/s00018-012-1032-3
- Riffelmacher T, Simon AK. Mechanistic roles of autophagy in hematopoietic differentiation. *Febs J*. 2017;284:1008–1020. doi:10.1111/febs.13962
- Cheung TH, Rando TA. Molecular regulation of stem cell quiescence. *Nat Rev Mol Cell Biol*. 2013;14:329–340. doi:10.1038/nrm3591
- Jacquel A, Obba S, Solary E, Auberger P. Proper macrophagic differentiation requires both autophagy and caspase activation. *Autophagy*. 2012;8:1141–1143. doi:10.4161/auto.20367
- Warr MR, Binnewies M, Flach J, et al. FOXO3A directs a protective autophagy program in haematopoietic stem cells. *Nature*. 2013;494:323–327. doi:10.1038/nature11895
- Song T, Wang H, Liu Y, Cai R, Yang D, Xiong Y. TPGS-modified long-circulating liposomes loading ziyuglycoside I for enhanced therapy of myelosuppression. *Int J Nanomedicine*. 2021;16:6281–6295. doi:10.2147/IJN.S326629
- Yongai Xiong YZ, Zhang D. Promotion of Ziyuglycoside I on white blood cells by autophagy pathway. *Chin Herb Med*. 2018;49:3350–3356.
- Xiong Y, Zou Y, Chen L, Xu Y, Wang S. Development and in vivo evaluation of ziyuglycoside I-loaded self-microemulsifying formulation for activity of increasing leukocyte. *AAPS PharmSciTech*. 2019;20:101. doi:10.1208/s12249-019-1313-3
- Fan J, Cheng Y, Sun M. Functionalized gold nanoparticles: synthesis, properties and biomedical applications. *Chem Rec*. 2020;20:1474–1504. doi:10.1002/tcr.202000087
- Zheng J, Cheng X, Zhang H, et al. Gold nanorods: the most versatile plasmonic nanoparticles. *Chem Rev*. 2021;121:13342–13453. doi:10.1021/acs.chemrev.1c00422
- Zhao P, Li T, Li Z, et al. Preparation of gold nanoparticles and its effect on autophagy and oxidative stress in chronic kidney disease cell model. *J Nanosci Nanotechnol*. 2021;21:1266–1271. doi:10.1166/jnn.2021.18655
- Zhou H, Gong X, Lin H, et al. Gold nanoparticles impair autophagy flux through shape-dependent endocytosis and lysosomal dysfunction. *J Mater Chem B*. 2018;6:8127–8136. doi:10.1039/C8TB02390E
- Ahmed HB. Recruitment of various biological macromolecules in fabrication of gold nanoparticles: overview for preparation and applications. *Int J Biol Macromol*. 2019;140:265–277. doi:10.1016/j.ijbiomac.2019.08.138
- Tao R, Wang C, Lu Y, et al. Characterization and cytotoxicity of polyphenol lipid and vitamin E-TPGS hybrid nanoparticles for betulinic acid and low-substituted hydroxyl fullerene in MHCC97H and L02 cells. *Int J Nanomedicine*. 2020;15:2733–2749. doi:10.2147/IJN.S249773
- Fast EM, Spoorij A, Manning M, et al. External signals regulate continuous transcriptional states in hematopoietic stem cells. *Elife*. 2021;10. doi:10.7554/eLife.66512
- Berköz M, Yalın S, Özkan-Yılmaz F, et al. Protective effect of myricetin, apigenin, and hesperidin pretreatments on cyclophosphamide-induced immunosuppression. *Immunopharmacol Immunotoxicol*. 2021;43:353–369. doi:10.1080/08923973.2021.1916525

20. Dong S, Wang Q, Kao YR, et al. Chaperone-mediated autophagy sustains haematopoietic stem-cell function. *Nature*. 2021;591:117–123. doi:10.1038/s41586-020-03129-z
21. Chen X, He Y, Lu F. Autophagy in stem cell biology: a perspective on stem cell self-renewal and differentiation. *Stem Cells Int*. 2018;2018:9131397. doi:10.1155/2018/9131397
22. de Haan G, Lazare SS. Aging of hematopoietic stem cells. *Blood*. 2018;131:479–487. doi:10.1182/blood-2017-06-746412

International Journal of Nanomedicine

Dovepress

Publish your work in this journal

The International Journal of Nanomedicine is an international, peer-reviewed journal focusing on the application of nanotechnology in diagnostics, therapeutics, and drug delivery systems throughout the biomedical field. This journal is indexed on PubMed Central, MedLine, CAS, SciSearch®, Current Contents®/Clinical Medicine, Journal Citation Reports/Science Edition, EMBase, Scopus and the Elsevier Bibliographic databases. The manuscript management system is completely online and includes a very quick and fair peer-review system, which is all easy to use. Visit <http://www.dovepress.com/testimonials.php> to read real quotes from published authors.

Submit your manuscript here: <https://www.dovepress.com/international-journal-of-nanomedicine-journal>